OBSERVATION OF INSULATION MECHANISM DURING FBTIG

Louriel O. Vilarinho, vilarinho@mecanica.ufu.br
Laprosolda, Federal University of Uberlandia, Av. João Naves de Ávila, 2121, Uberlândia/MG, 38400-902, Brazil

Sayee Raghunathan, Sayee.Raghunathan@twi.co.uk
Bill Lucas, Bill.Lucas@twi.co.uk
The Welding Institute, TWI Limited, Granta Park, Great Abington, Cambridge, CB21 6AL, United Kingdom

Abstract. *The penetration increase reached in TIG welding by applying active flux on the workpiece surface, unfolding a process namely A-TIG, presents a version of applying the flux aside of the final weld bead. This technique known as FBTIG (Flux Bonded TIG) is claimed to achieve the same benefits of penetration enhancement of the A-TIG process (with the flux spread over the final bead), but with a better quality of the bead surface, i.e, lower presence of slag formed from the flux. Although its high technological importance, the FBTIG is not fully understood, especially the mechanisms behind the penetration increase. Therefore, in order to contribute to the understanding of this mechanism, a series of runs were performed on austenitic stainless steel, while the weld pool was filmed by a dedicated vision system capable of getting rid of the arc light and imaging only the weld pool, electrode, workpiece and formed bead. Also the electrical signals (voltage and current) were acquired. From the analyses, it is possible to conclude that the flux acts as an insulation barrier, interfering in the arc magnetic/electrical field. This feature constricts the arc, increasing the electromagnetic force and, therefore, the plasma jet, which, in turn, leads to the penetration enhancement. It is also shown that this mechanism does not take place in the A-TIG welding.*

Keywords: Welding, Penetration Enhancement, Active Flux.

1. INTRODUCTION

Despite the intrinsic advantages of the TIG process in welding fabrication, such as high quality, smooth bead profile, and low-distortion, it still lacks of high productivity and limited thickness that can be welding in single pass operations. Among the different approaches, which have been proposed to solve these limitations, one specific technique has been shown affordable, robust and efficient calls the attention. It is the use of active flux over the workpiece prior welding and carrying the arc over it (A-TIG – Active Flux Tungsten Inert Gas) or aside it (FBTIG – Flux Bonded Tungsten Inert Gas), as shown in Fig. 1.

The A-TIG welding has been successfully shown as an efficient process variant for penetration enhancement. However, the presence of slag on the top of the bead reduces the bead surface quality. Therefore, the FBTIG process arises as a very important option to overcome the mentioned limitation and, at the same time, keep the bead surface quality. The main reason for the better bead surface is that the flux is spread on both sides of the joint and not over the joint itself (as the A-TIG is carried out).

Even with this great technological contribution to the welding fabrication, the fully understand of the mechanisms behind the penetration increase has not been reached. Therefore, it is proposed here to perform an initial investigation on the phenomena behind the FBTIG by observing the weld pool images from an infrared vision system, when the arc approximates to a flux coating in a austenitic stainless steel plate. It is expect that, from a better understand of the mechanisms involved in the A-TIG process, it could lead to further development in the flux composition, application technique and specific flux for different materials.
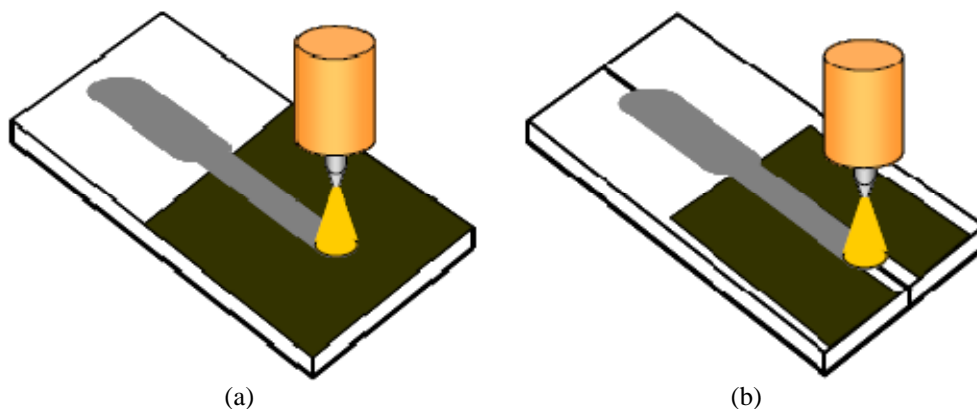

Figure 1. Schematic view of the (a) A-TIG and (b) FBTIG processes (after Richetti, 2003).

1.1. Constriction mechanism

The main mechanism claimed on literature to be responsible for the resulting effect of penetration increase when the flux is applied aside of the joint is the arc contraction. This contraction in the electric arc reduces its area, increasing the current density and, therefore, increases the penetration. This is done since the flux coating acts as an electric insulator (Marya, 2004). This theory has been investigated numerically (Lowke et al., 2004 and 2005) and a very strong sign of its veracity is presented on the work of Richetti (2003), where ordinary sand (from the soil) was capable of acting as a FBTIG flux.

This theory can be summarised on Fig. 2. In this figure, it is shown the three main dimensions that characterise an electric arc: its electric radius, the optical radius and the anode spot. In Fig. 2a, it is shown a schematic view of the arc and its interaction with a flux layer and in Fig. 2b the measured values for a 150-A arc in a pure-Ar TIG welding. From Fig. 2b it is possible to predict that the electric arc will interact with barriers place at a distance as far as 20 mm (in this particular case). Since the flux normally employed are good electrical insulator (Vilarinho et al., 2009a), it is reasonable to assume that it acts as a barrier (insulation) and tends do reduce de arc diameter due to the change in its electromagnetic field.
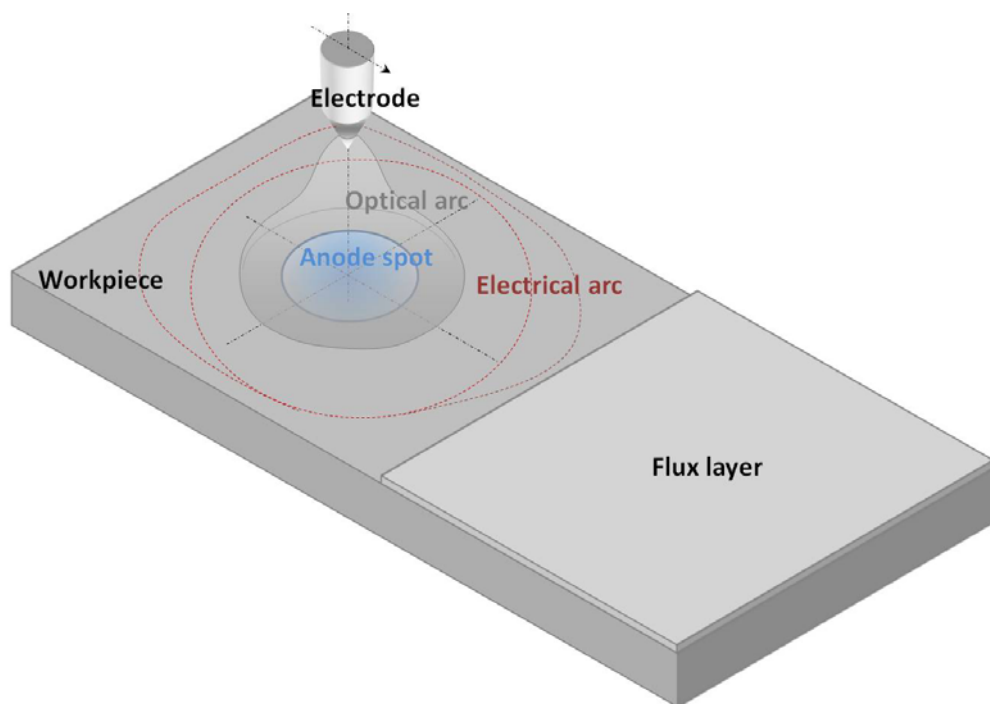
(a)
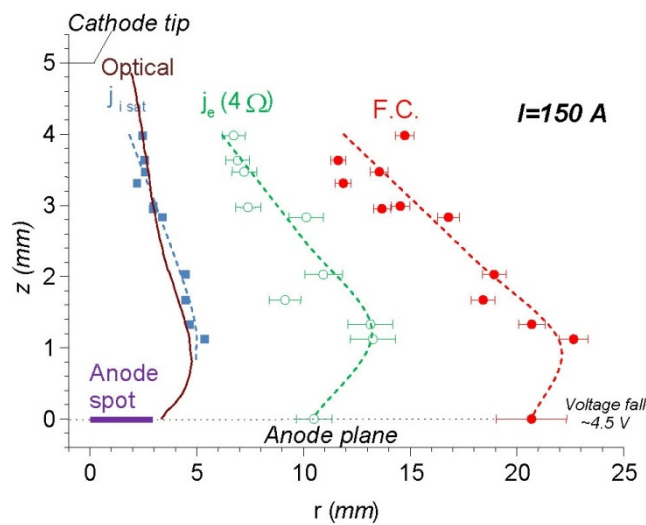
(b)

Figure 2. (a) General idea of different arc dimensions to be considered and (b) measured values by Vilarinho (2002) in a 150-A, Ar, TIG, 5-mm arc length and WTh2 3.2-mm electrode: j_{isat} is the ionic saturation current, j_e is the electronic saturation and F.C. is where the floating condition is reached by an electrostatic probe.

Although, this theory seems plausible, it has not been confirmed. Therefore, it is aimed to look for phenomena that confirm this theory by using a dedicated vision system (Vilarinho, et al., 2009b) to visualize the weld pool when the arc interacts with the flux layer and also use digital image processing to abstract quantitative information from those images.

2. EXPERIMENTAL APPROACH

2.1. Material

Austenitic stainless steel SUS304 was selected and plate dimension of 125 x 38 x 4.7 mm was cut by guillotine, considering both heat flow and availability. The plate size is important because it could influence the bead geometry. Bigger plates promote fast cooling rates, which could emphasize the penetration-increase effect (more localized heat).

2.2. Equipments and parameters

The experimental rig consists of an inverter power source was used with a TIG torch water cooled moving at 1.7 mm/s, electrode W+2%Th (diameter 2.4 mm) and an arc length of 3 mm. The nozzle inner diameter is 10 mm and the electrode stick-out is 10 mm. In fact, this is the maximum recommend in practical literature (equal to the nozzle diameter). Commercial pure Argon at 12 l/min was used. The acquisition system was set at 1 kHz per channel for voltage and current record.

The 150-A current was selected from preliminary tests where full penetration was achieved while on flux and partial penetration when out of it. In order to compare current levels, one experiment at 100 A was proposed. The travels speed was selected as 1.0 mm/s from the calculation of temperature distribution using Rosenthal's procedure, in order to keep the temperature distribution over the plate approximately the same between 150 and 100 A.

2.3. Vision System

The vision system is an essential tool for the weld pool visualisation on the search for the mechanism. It comprises a Diode Laser Type IIIB. This diode laser array illuminates the weld-pool area at 905 nm wavelength light and demands a CCD camera with infrared sensitivity. The final frame rate of the camera was 20.9 fps.

The maximum number of frames capable with the currently hardware is 1917 frames. Therefore, for the length of the bead used here, 1.7 mm/s of travel speed is the lowest value that guarantees flexibility without data loss.

2.4. Flux Application Technique

The flux used in this work consists of a mixture of silicate salts that has been employed technologically at The Welding Insitute - TWI (Howse & Lucas, 1997). A spray gun (model 250-3 Airbrush from Badger) was used for spraying the flux over the plate. The air pressure was kept constant and the air quality is considered as a standard industrial line at 3 bar. The distance from the plate to the spray nozzle was kept constant at 100 mm and the travel speed at ~50 mm/s (manual application). The thickness of the coating after the flux is dried was measured by a coating thickness gauge (PosiTestDFT, 2004), which has a range of 0-1000 microns and accuracy of ±2 microns + 3%.
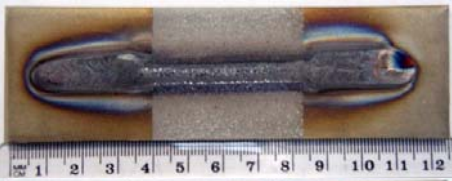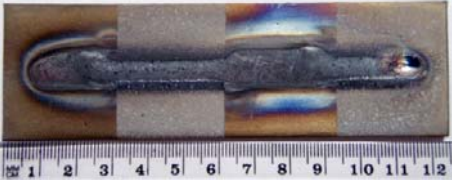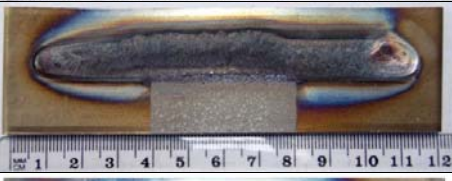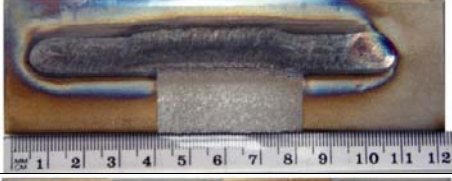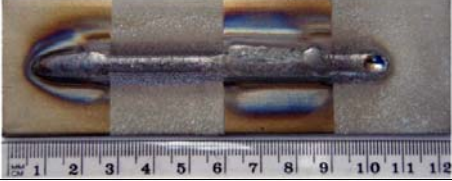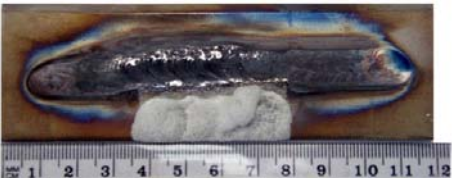
These approaches lead to a consistent and repeatable 7-9 microns coating thickness. Since the flux was kept at the same composition, the amount of flux can be considered as the same. It must be pointed out that the proposed approach led to satisfactory results, since the accuracy of the gage is higher than the deviation standard of the measured thicknesses.

3. RESULTS AND DISCUSSION

From the proposed experimental approach 6 runs were carried out according to Tab. 1, where it is shown the flux layer distribution, current levels, travel speed, thickness of the flux layer, measured average voltage (in this case, equal to the rms one) and final bead appearance. It must be point out the analysis of the FBTIG will be characterized by the images directly from R03, R04 and R06. The other runs will be analysed when the electric arc and electrode reach the flux interface and leave it and not inside the flux layer (otherwise, it would be A-TIG process).

The first image from this idea of analysing the interface is shown in Fig. 3 for run R01. It shows the voltage falling due to the presence of lower ionisation elements in the flux formulation (Vilarinho et al., 2009a). Moreover, a series of images are shown in Fig. 4 for run R06, where the weld pool disturbance are shown, especially the weld pool length, which tends to increase, when the weld pool gets closer to the flux layer. This observation corroborates to the idea that the flux acts as an insulation layer, blocking the movement of the weld-pool front and, therefore, pushing the molten metal back.

Table 1. Experimental runs and results.

Run	Current [A]	Travel speed [mm/s]	Flux thickness [microns]	Mean voltage [V]	Figures of face appearances
R01	150	1.7	8	11.3	
R02	150	1.7	8	11.1	
R03	150	1.7	8	12.0	
R04	150	1.7	16	11.7	
R05	100	1.0	8	10.8	
R06	150	1.7	100	11.8	
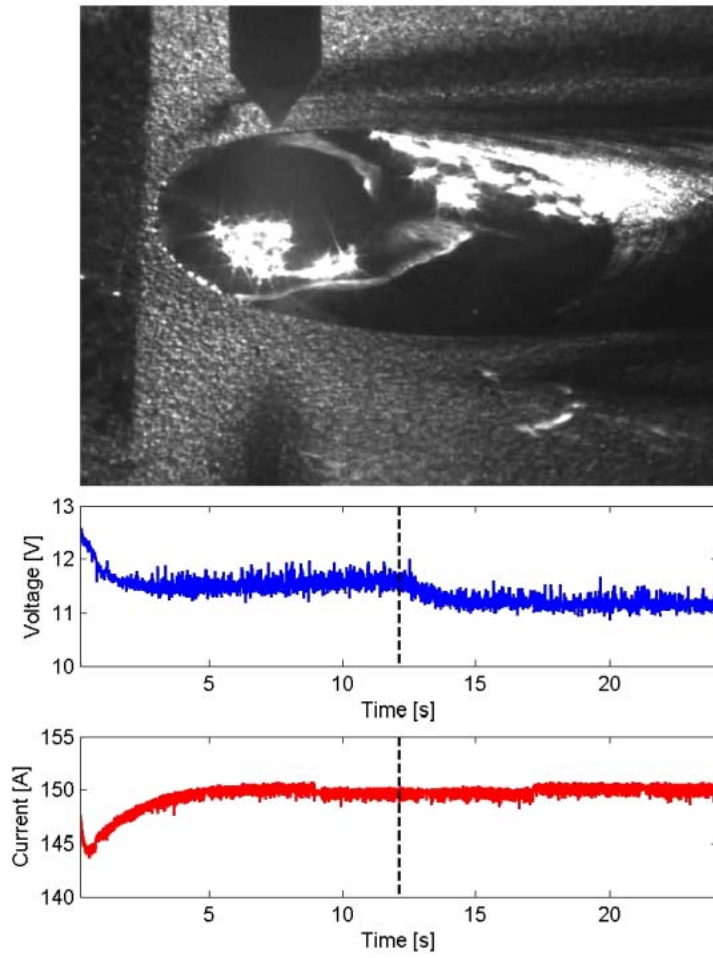
Figure 3. Weld pool reaches the flux interface for run R01 (Copyright © TWI Ltd).
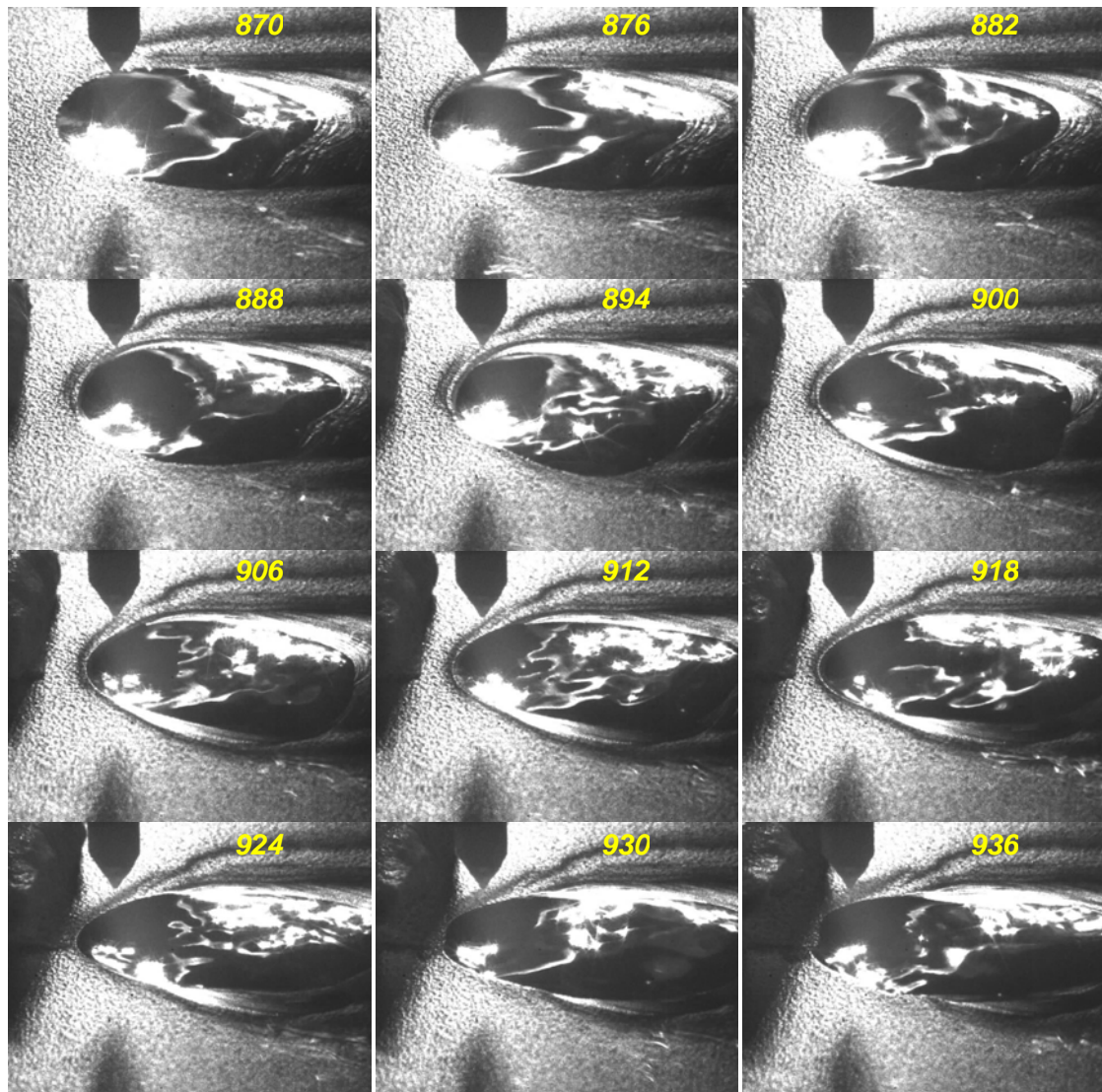
Figure 4. Image sequence showing flux influence on weld pool before contact between them (run R06). The numbers indicate the frame number, which time interval between one frame and other is ~ 48 ms (Copyright © TWI Ltd).

Using digital image processing tools is possible to calculate the evolution of the distance between the weld pool and the interface. If the assumption of insulation mechanism blocking the weld pool front is correct, than a reduction in the travels speed of the front must be noted. Figure 5 presents the measured values of the distances between the weld-pool front and the flux interface, as well as the distance between the electrode tip and the flux interface. The idea of the first measurement is to confirm the theory, whereas the second one aims to check if the procedure is correct. If it is, then a straight line must appears representing the travel speed (1.7 or 1.0 mm/s, depending on the run).

Both curves of Fig. 5 match their objective, i.e., the blue curve (distance between the weld-pool front and flux interface) presents a desacceleration starting at ~1.25 s, whereas the red curve (distance between the electrode tip and flux interface) is a straight line with a slope equal to 1.66 mm/s.

This same trend is observed in Fig. 6 for the run R02, which is basically a repetition of run R01 for confirming the theory, and Fig. 7 for run R05, which means that the phenomenon happens at different welding currents.

A further confirmation of the insulation mechanism theory can be found in Figs. 8 and 9. If the assumption of pushing back the molten metal when it reaches the flux interface is true, the assumption of pushing forward the molten metal when it leaves the flux layer must be also true. This is confirmed in both Figs 8 and 9, for runs R02 and R05, respectively. On Fig. 8 at ~4.5s, the weld-pool front accelerates. The same trend can be seen at ~2.75 s on Fig. 9. It also confirms that the insulation mechanism happens at different current levels.

Moreover, a final observation of the phenomenon can be seen in Fig. 10 and 11 for runs R03 and R04, respectively. The weld pool deviation is clearly seen on the images. The molten metal is pushed away of the flux layer.
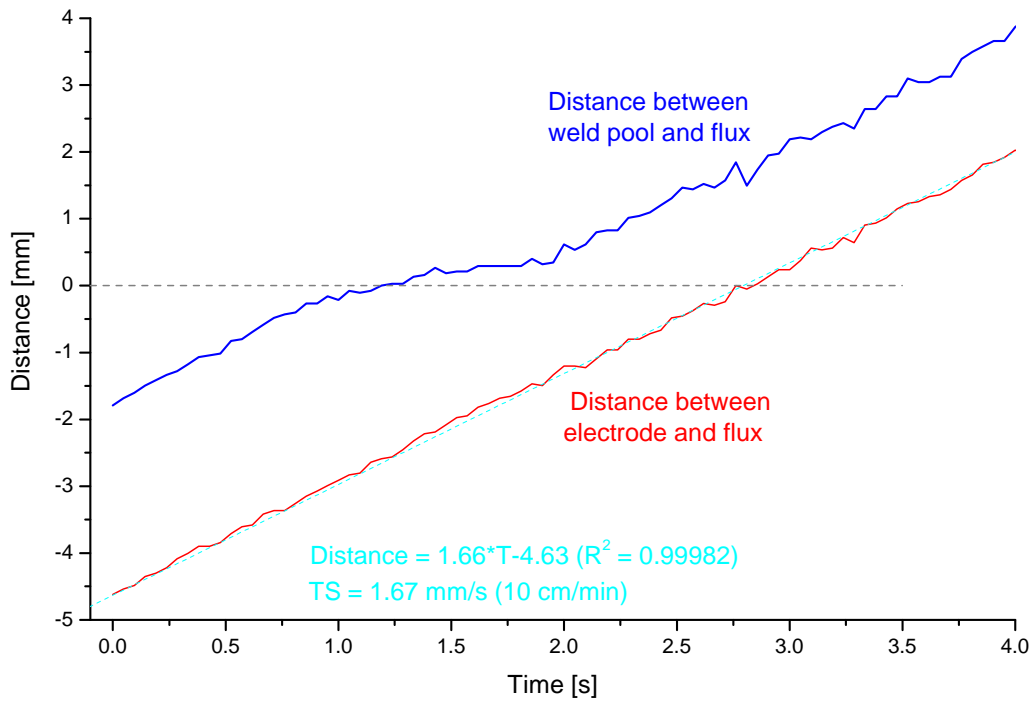
Figure 5. Distances between the weld pool-flux and electrode-flux for run R01 (Copyright © TWI Ltd).
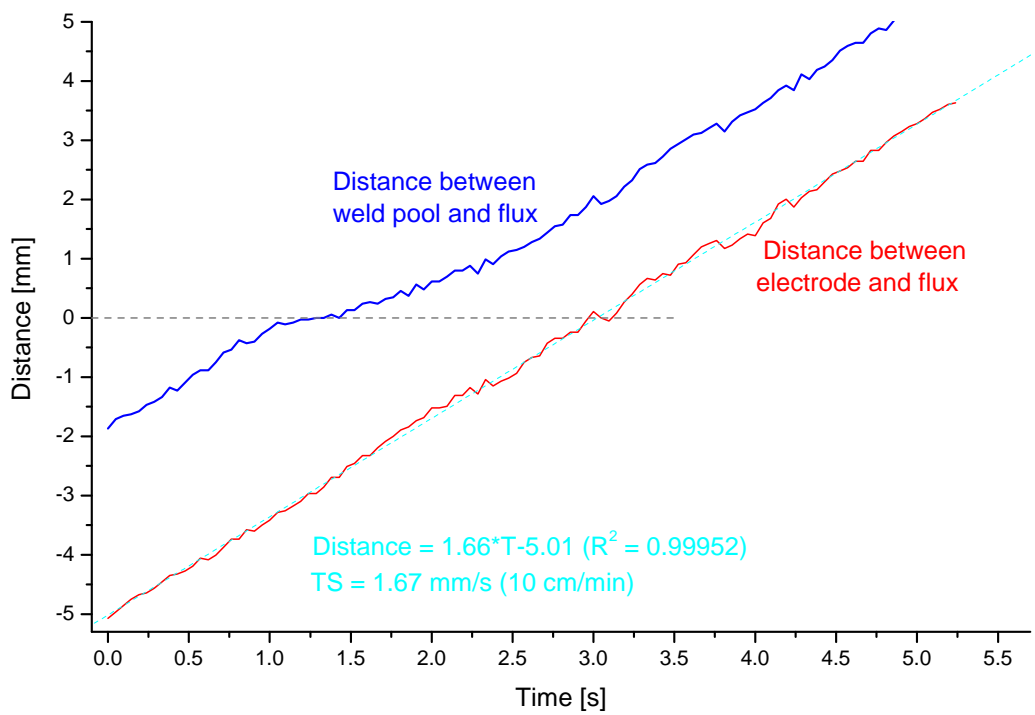

Figure 6. Weld pool length and distances between the weld pool-flux and electrode-flux for run R02, when the arc enters into the flux (Copyright © TWI Ltd).
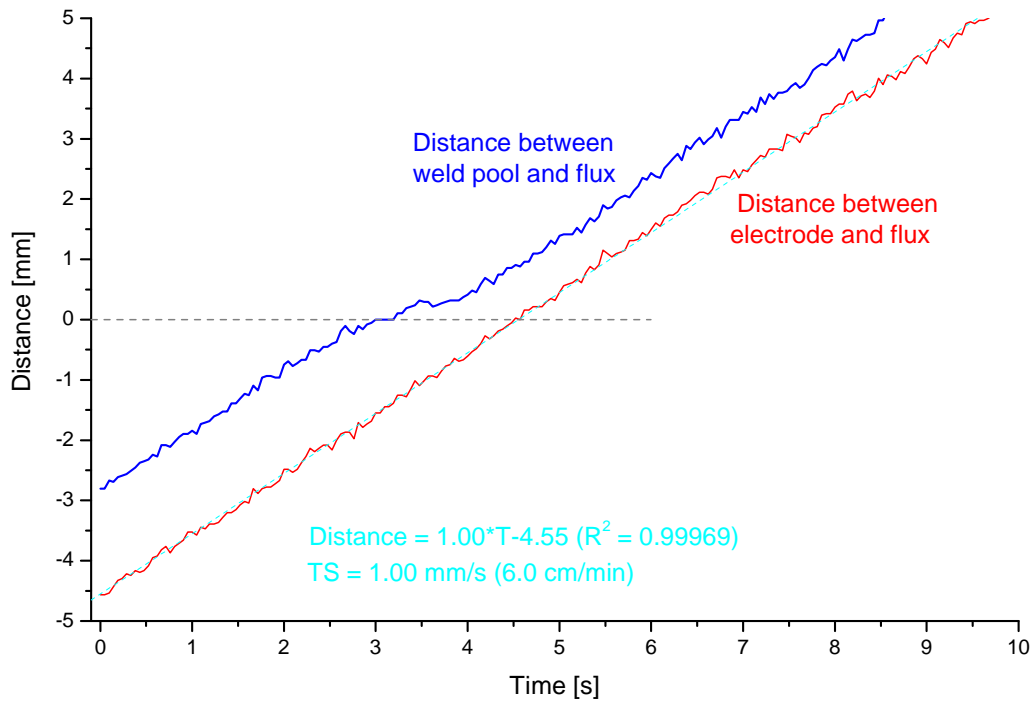
Figure 7. Weld pool length and distances between the weld pool-flux and electrode-flux for run R05, when the arc enters into the flux (Copyright © TWI Ltd).
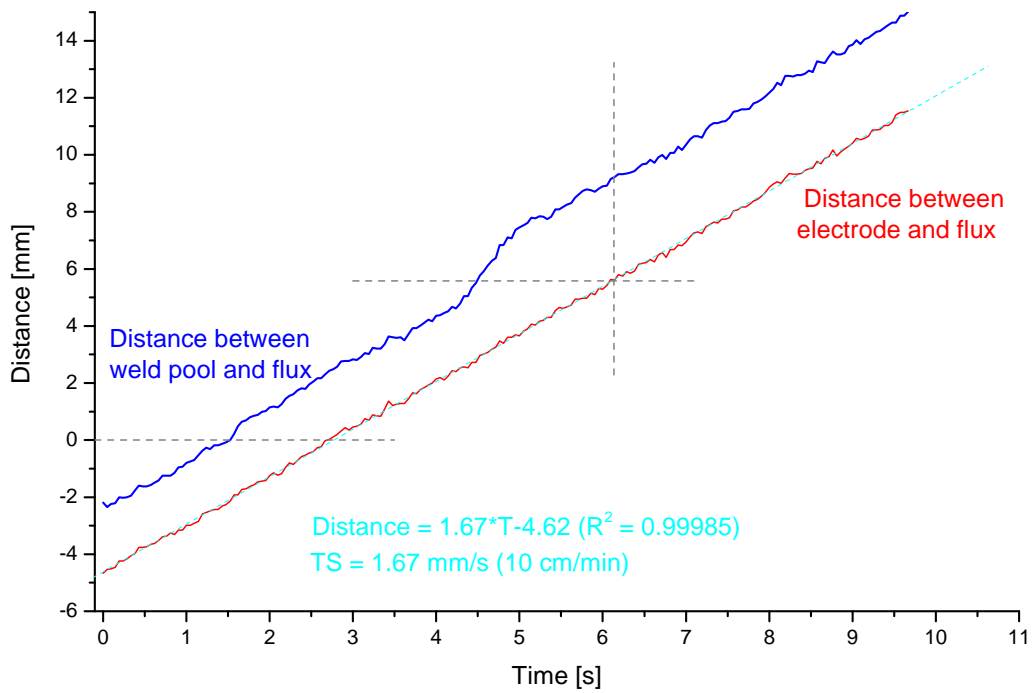

Figure 8. Weld pool length and distances between the weld pool-flux and electrode-flux for run R02, when the arc comes out the flux (Copyright © TWI Ltd).
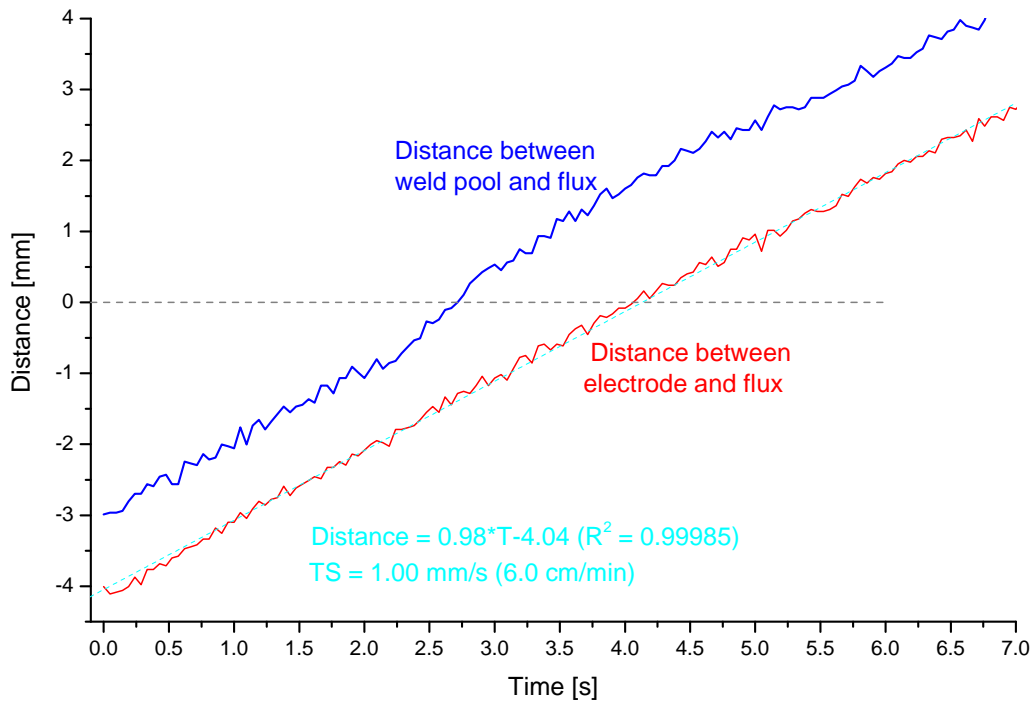
Figure 9. Weld pool length and distances between the weld pool-flux and electrode-flux for run R05, when the arc comes out the flux (Copyright © TWI Ltd).
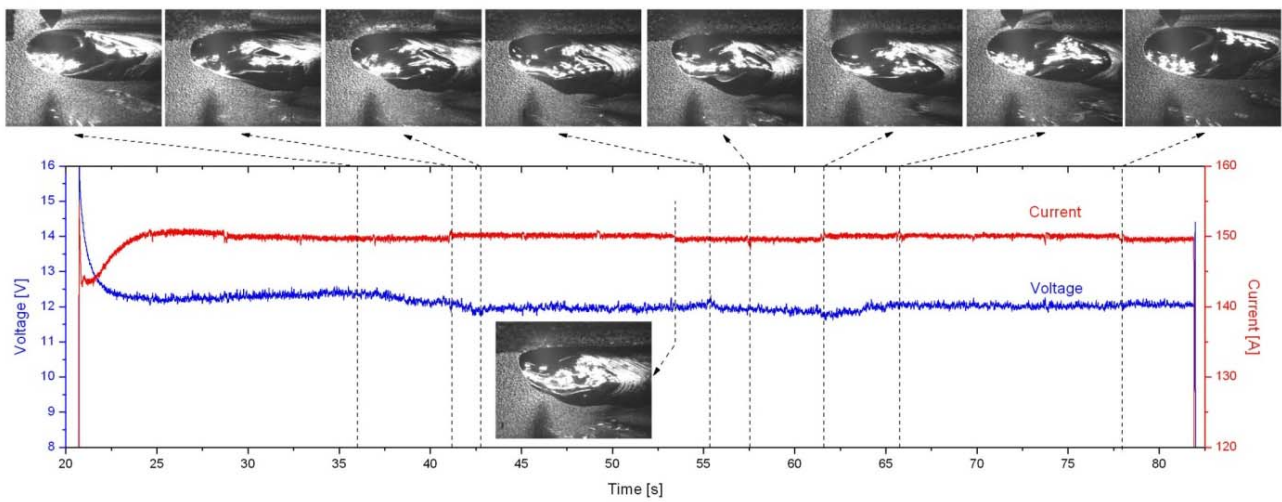

Figure 10. Images synchronised with electrical signals for run R03 (Copyright © TWI Ltd).
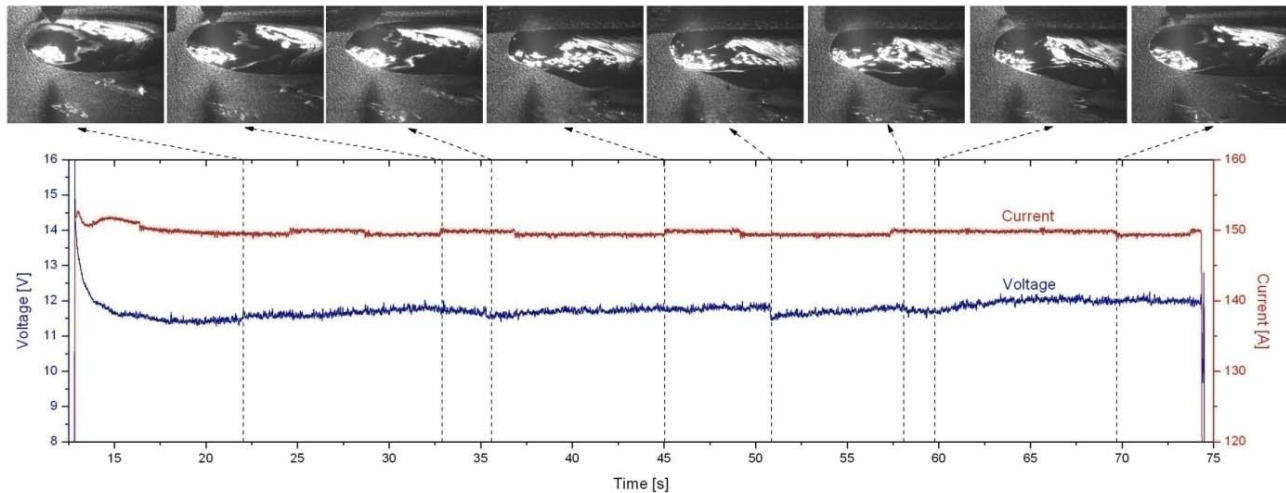
Figure 11. Images synchronised with electrical signals for run R04 (Copyright © TWI Ltd).

4. CONCLUSION

The main mechanism behind the FBTIG effect of penetration increase seems the insulation effect provided by the flux layer. It acts constricting the weld pool and, since the current is kept constant, increases the current density, and, finally, the penetration.

5. ACKNOWLEDGEMENTS

Prof. Vilarinho would like to thank CAPES under project BEX 1535/08-0 and The Welding Institute for their support.

6. REFERENCES

Howse, D. S., W. Lucas, et al., 1997. "An Investigation into the Mechanisms of Active Fluxes for TIG (A-TIG) Welding", The Welding Institute Repot: 50.
PosiTestDFT, 2004. "Coating Thickness Gage - Instruction Manual ver. 1.0 (Combo - measures on all metals)", USA: 1p.
Lowke, J. J. et al., 2004. "Insulation Effects of Flux Layer in Producing Greater Weld Depth", IIW Doc: 7p.
Lowke, J. J. et al., 2005. "Mechanisms Giving Increased Weld Depth due to a Flux." J. Phys. D: Appl. Phys. 38: 3438-3445.
Marya, S. 2004. "Enhancing GTAW Performance Through Flux Coatings: Theoretical Background And Industrial Applications", IIW Doc, 9p.
Richetti, A., 2003. "Analysis and Empirical Modelling of PAW with Keyhole in Stainless Steel". PhD Thesis, FEMEC. Uberlandia, Federal University of Uberlandia, 292p.
Vilarinho, L. O., 2002. "Characterisation of TIG Arc Structures Using Experimental Techniques", Cranfield University Report, 325p.
Vilarinho, L.O. et al. 2009a. "Spectroscopic Measurement During A-TIG Welding of Austenitic Stainless Steel", Submitted to the COBEM2009, Gramado/RS, Brazil.
Vilarinho, L.O. et al. 2009b. "Dedicated Infrared Vision System for Monitoring Welding Processes", Submitted to the COBEM2009, Gramado/RS, Brazil.

7. RESPONSIBILITY NOTICE

The authors are the only responsible for the printed material included in this paper.